2006

Synthesis and analysis of an α-amylase inhibitor and an antimicrobial peptide

Brahmlin Kaur Sethi

Synthesis and analysis of an α-amylase inhibitor and an antimicrobial peptide

Abstract

Abstract 1: α-Amylase is an important enzyme in the body responsible for hydrolyzing many polysaccharides such as dietary starch. Inhibition of this enzyme could be extremely beneficial in diabetic patients because it could lower the glucose levels in the blood. Our objective is to synthesize a small analog of a natural α-amylase inhibitor, Tendamistat. This molecule has 15-22 residue segment that are critical for its activity. The peptide was synthesized, cleaved, purified, analyzed, and an enzyme assay was run. Michaelis Menton and Lineweaver-Burk plots were constructed to determine the V_{max}, K_m, and K_i for each assay and determine the activity. It was determined that the assays yielded inconclusive data, and therefore, it could not be determined whether competitive inhibition was occurring. Also the K_is for the synthesized peptide and the native peptide were extremely different which also tells us that this is not going to be a useful drug for diabetic patients.

Abstract 2: The LL-21 is the smallest active sequence for the antimicrobial LL-37 peptide. Were LL-37 is a natural human immune defense and uses a different mechanism (drugs like penicillin which only attack bacteria during reproduction state) of entry into the bacterial cell wall. The research consisted of determining the activity of LL-21 against different bacterial strains. The methods to determine its activity were to synthesize, cleave, purify, and then send peptide to our U of M sponsor to analyze. The peptide was found to be active in the 0.4 to 100 µg/ml range. Further studies would use isotopically labeled groups on the peptide and be studied thoroughly by the NMR to find the mechanism of action.

Degree Type

Open Access Senior Honors Thesis

Department

Chemistry

Keywords

Diabetes Research, Peptides, Amylases Inhibitors

Subject Categories

Chemistry

Synthesis and Analysis of an α-Amylase Inhibitor and an Antimicrobial Peptide

By
Brahmlin Kaur Sethi

A Senior Thesis Submitted to the
Eastern Michigan University
Honors Program
In Partial Fulfillment of the Requirements for Graduation with Honors in Chemistry

Approved at Ypsilanti, Michigan, On this date _____

_____
Supervising Instructor (Print Name and have signed)

_____
Honors Advisor (Print Name and have signed)

_____
Department Head (Print Name and have signed)

_____
Honors Director (Print Name and have signed)

Table of Contents

Abstract 1: α-Amylase is an important enzyme in the body responsible for hydrolyzing many polysaccharides such as dietary starch. Inhibition of this enzyme could be extremely beneficial in diabetic patients because it could lower the glucose levels in the blood. Our objective is to synthesize a small analog of a natural α-amylase inhibitor, Tendamistat. This molecule has 15-22 residue segment that are critical for its activity. The peptide was synthesized, cleaved, purified, analyzed, and an enzyme assay was run. Michaelis Menton and Lineweaver-Burk plots were constructed to determine the V_{max}, K_m, and K_i for each assay and determine the activity. It was determined that the assays yielded inconclusive data, and therefore, it could not be determined whether competitive inhibition was occurring. Also the K_is for the synthesized peptide and the native peptide were extremely different which also tells us that this is not going to be a useful drug for diabetic patients.

Abstract 2: The LL-21 is the smallest active sequence for the antimicrobial LL-37 peptide. Were LL-37 is a natural human immune defense and uses a different mechanism (drugs like penicillin which only attack bacteria during reproduction state) of entry into the bacterial cell wall. The research consisted of determining the activity of LL-21 against different bacterial strains. The methods to determine its activity were to synthesize, cleave, purify, and then send peptide to our U of M sponsor to analyze. The peptide was found to be active in the 0.4 to 100 μg/ml range. Further studies would use isotopically labeled groups on the peptide and be studied thoroughly by the NMR to find the mechanism of action.

Introduction

I worked on two projects this year for my undergraduate research. One of them focused on α-amylase inhibitors and their activities which could be beneficial for diabetics. The other was to synthesize the smallest and most active sequence of the antimicrobial peptide LL-37 and understand the molecular basis of its membrane disruption.

Introduction to α-amylase and Tendamistat research

Alpha-amylase enzyme catalyzes the endohydrolsis of α (1->4) glycosidic linkages in common polysaccharides (starches) from the diet, to regulate blood sugar levels (Figure 1). During the disease state of diabetes mellitus, this enzyme can be detrimental, due to the biochemical defect causing blood glucose levels to be elevated. Inhibition of the enzyme's activity would lower glucose absorption by the small intestine and would control the elevation of glucose levels. This would then allow more undigested starch to make it to the colon.

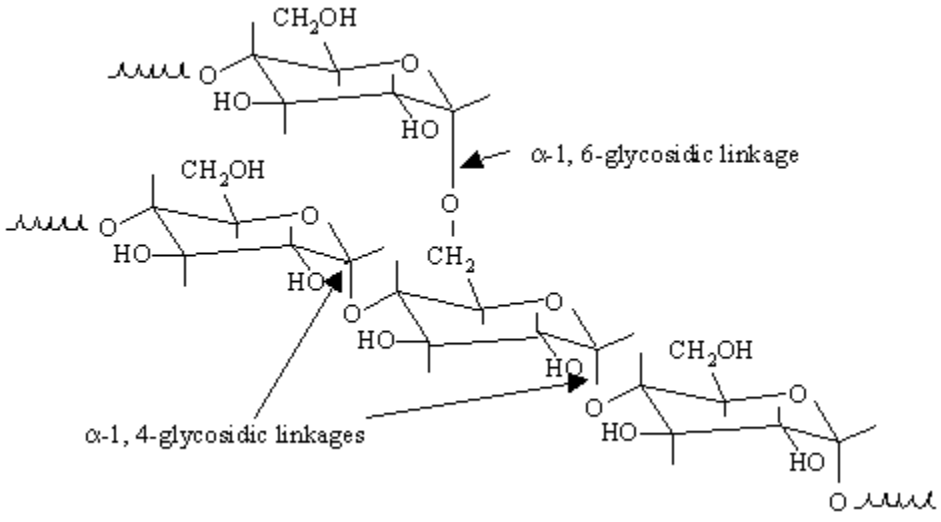

Figure 1: The polymeric structure of glucose in starch tends to be formless (1).

The goal of the project was to develop a small peptide drug based on the natural analog, Tendamistat. Tendamistat is a tight-binding 74 amino acid long protein that specifically inhibits mammalian α-amylase (Figure 2). To better understand the structural, conformational, and molecular-level interactions, it might be better to study smaller analogs of Tendamistat.

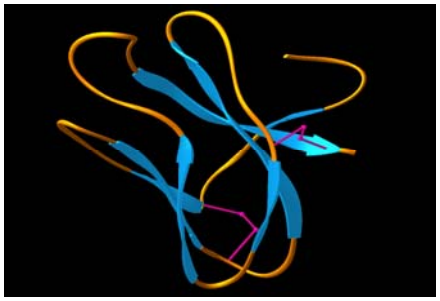

Figure 2: is the 74 amino acid long Tendamistat, The only secondary structure found in the protein are six beta sheets shown here in blue. The protein also contains two disulfide bridges; Cys11-Cys27 and Cys45-Cys73 which are shown in pink (2).

This protein inhibitor was isolated from Streptomyces (expressed on surface of the filamentous bacteriophage M13), of which only 8 amino acids are essential for the inhibitor's direct interaction with the enzyme binding site, which are Tyr-Gln-Ser-Trp-Arg-Tyr-Ser-Gln (Figure 3). This was discovered by x-ray crystallography and nuclear magnetic resonance (3,4). This work suggests that a small portion of this peptide is responsible for binding to the novel site.

Tendamistat is a pseudo-irreversible inhibitor of mammalian α-amylase with a K_i value of 9×10^{-12} M (5). Topographical changes are induced in the enzyme, but not in the inhibitor, upon binding (5). There is a 1:1 stoichometric complex between Tendamistat and the enzyme which blocks the access of glycogen or starch, therefore

stopping the enzyme's functionality. Further computational studies have modeled the α-amylase-Tendamistat complex and discovered that approximately 30% of the inhibitor's water accessible surface area is in contact with the enzyme (5). The disulfide bonds formed by Cys^{11} and Cys^{73} in Tendamistat are crucial for the inhibitor's activity, since they give rise to the smaller loop. The inhibitor has 15 important amino acids responsible for direct interaction with the enzyme binding site via hydrogen/ hydrophobic bonding and electrostatic forces (segments shown below) (6).

Segment 1: Tyr^{15} Trp^{18} Arg^{19} Tyr^{20}

Segment 2: Leu^{44} Tyr^{46}

Segment 3: Gln^{52} Ile^{53} Thr^{54} Thr^{55}

Segment 4: Asp^{58} Gly^{59} Tyr^{60} Ile^{61} Gly^{62}

Segment 1 is responsible for binding at the catalytic site and blocking the natural substrates while the other segments contribute to the recognization of specific α-amylases. Segments 1 and 3 are responsible for β-sheet structure, while segment 2 is involved with a partial β-sheet, stabilized by disulfide bonds. Segment 4 helps stabilize the β-turn of the crucial triplet by being adjacent to segment 1 (6).

The critical residues used in our analogs from Tendamistat are from 15-22. This is an important sequence because of Tyr^{15} which loops around to hydrogen bond with Gln^{22} and is important for mammalian activity. Specifically the Trp^{19}, Arg^{20}, and Tyr^{21} form a β-turn in Temdamistat such that the large positive side chain by the N-terminus is able to loop out and interact with the enzyme (negative charge on amylase interacts with the positive charge on Arg^{20}) (5).

There are several reasons why developing a smaller analog is beneficial. First, a large molecule has detrimental side effects and may trigger an immune response, which could cause the patient harm. Next, digestive enzymes could attack the natural protein because it lacks novel amino acids and the drug would never reach its target. Even though Tendamistat is resistant to hydrolases and denatures only at temperatures as high as 90°C (5), additional unnatural amino acids incorporated into the sequence could give it additional protection. Also smaller peptides are less costly for large scale production. Lastly smaller sequence are easily studied structurally and more readily modeled. Since Tendamistat is a well studied protein it is advantageous in determining a general small analog which will be able to mimic the larger one. This could ultimately be a pharmaceutical drug that would be beneficial to patients with diabetes mellitus whether young or old. Also, this drug might have another type of mechanism from typical polysaccharides inhibitors.

Small analogs that mimic a macromolecule in conformational and physicochemical characteristics may also mirror its binding properties. Other studies have been performed to minimize the Tendamistat sequence. The peptide c(D-Pro-Phe-Ser-Trp-Arg-Tyr) gave a K_i value of 14μM,while if Ser was replaced by Ala it gives the value 32 μM. Linear tri-to hexapeptides bound with weaker affinity; the best, Ac-Trp-Arg-Tyr-OMe acts as a competitive inhibitor with an inhibition constant of 100 μM (5).

The significance of this study is that about 8 million Americans suffer each day from diabetes mellitus. Even though there are other treatments such as insulin therapy, diet, hyperglycemic agents, and other drugs, other agents would be useful. The related complications for diabetes mellitus have been a result of hyperglycemia, which affects

vascular permeability, blood flow, as well as nerve transmission (5). Consequently, by reducing hyperglycemia, a drug could slow down or reverse processes in retinal, kidney, nerve, and vascular tissue. This work might lead to a peptidomimetic drug or foundation for treatment. These studies could further develop our grasp on molecular interactions at the α-amylase active site, which may lead to other research and development of other ligands.

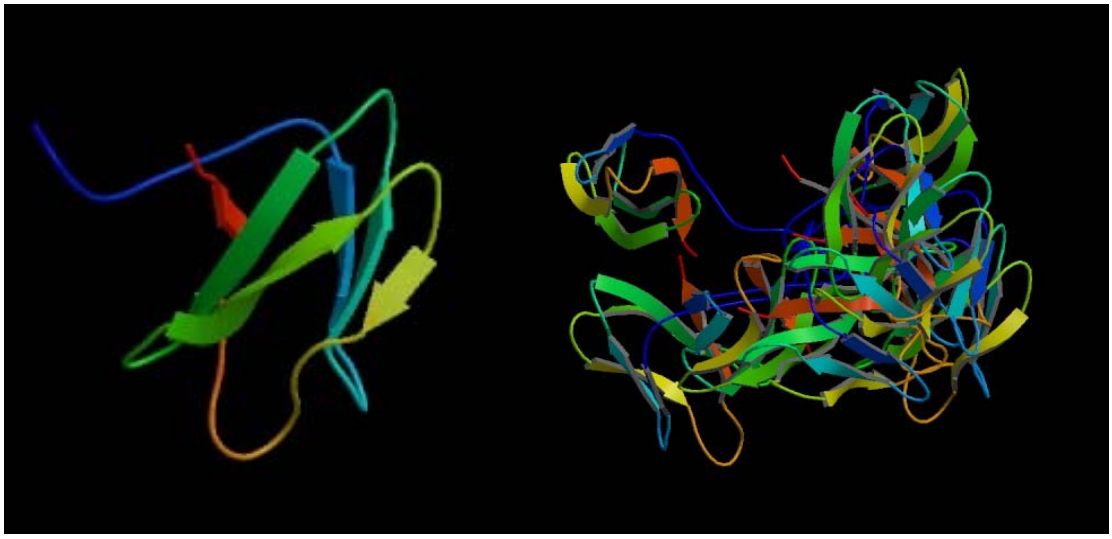

Figure 3: Restrained energy refinement with two different algorithms and force fields of the structure of the alpha-amylase inhibitor Tendamistat determined by NMR. The figure to the right is the Tendamistat in aqueous solution by nuclear magnetic resonance and distance geometry (4).

Tendamistat must be broken down into a smaller sequence because otherwise it will be destroyed by the immune system network due to its massive size. This is why it is broken down for potential drugs into smaller analogues that contain the key amino acids. The most effective analogue developed in our lab thus far is NFH-1 (K_I = 6.7 x 10^{-5} M), which is (Ac)-Tyr-Gln-Ser-Trp-Arg-Tyr-Ser-Gln-(NH_2). Note the serine residues present on either side of the key triplet; this gives rise to hydrogen bonding

capability intramolecularly and intermolecularly, but the hydroxyl group can effect side reactions. The side reactions (interaction with other agents and no loop formation into preferred pattern) could cause the inhibitory activity to be altered and lead to ineffective pharmaceutical activity (5). The same is true for the hydroxyl group on the Tyr residue (Figure 4).

This parent analog (Tendamistat 15-22) was slightly altered and synthesized as p-NH_2Phe-Gln-Ser-Trp-Arg-Tyr-Ser-Gln (figure 3). This sequence should also attain additional hydrolytic stability, leading to enhanced bioavailability, and alternative folding patterns. The first residue has an NH_2 on the para position of the phenyl ring instead of a hydroxyl group, as would be found on the natural tyrosine. The amine group was chosen because it has similar characteristics as the OH on the Tyr. Observation of the activity of the amine group at this position and how it compared to the OH group was accomplished by enzyme assays. It was suspected that a similar H-bonding pattern would allow the required β turn loop, which is crucial to its activity, but the amine may be less reactive with other species. (5)

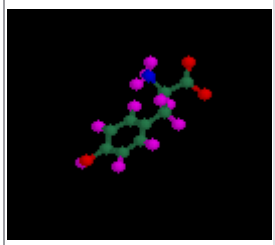	Tyrosine	Tyr	Y	aromatic polar hydrophobic	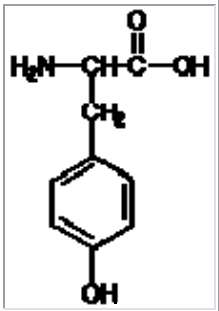

Figure 4: The tyrosine residue with its Rasmol image, 3 and 1 letter code, properties and structure (3).

Our sequence as shown previously is p-NH_2Phe-Tyr-Gln-Ser-Trp-Arg-Tyr-Ser-Gln, where we added the NH_2 to the para position on Phe instead of the OH in Tyr. The resulting peptide was tested for activity using spectrophotmetric analysis and Lineweaver-Burk plots were used for K_I calculation and comparison.

Introduction to LL-21 research

The other project is based on the LL-37 sequence from the human defense system. LL-37 is naturally expressed in neutrophils and epithelial tissues in humans. This is the first line of defense against bacterial infections, which is accomplished by destroying bacterial membranes through either a detergent-like mechanism (Figure 5) or pore formation. The carpet or detergent mechanism would show the LL-37 attacking the bacterial cell wall, deteriorating it by surrounding its lipids in a micelle, and sending the pieces off to macrophages to be released from the body. This means that the peptide molecules surround and pull apart the membrane lipids, destroying the membrane structure of bacteria. The other mechanism shown is the barrel-stave, which disrupts the cell was by placing multiple LL-37 molecules in a circular form throughout forming pores through which the cell contents can escape. This works because the hydrophobic part allows for penetration of the lipid membrane, disrupting membrane structure by creating many holes, resulting in cell death. These transmembrane pores upset the electrochemical gradient which leads to osmosis and cell rupture. These mechanisms are suggested to be due to the amphipathic sequence of LL 37 (polar/nonpolar mix). The positive charge of arginine and lysine residues attract specifically to bacterial membranes, because of the bacteria's negatively charged phosphatidyl esters (P.E.) (8). The

mammalian cell membranes contain more positively charged phospholipids so do not attract the peptide. This mechanism of attack may be helpful in drug discovery since it focuses on bacterial cells when not replicating and is unlike any other method thus far on the drug market. Also the bacteria should not acquire resistance to this mechanism.

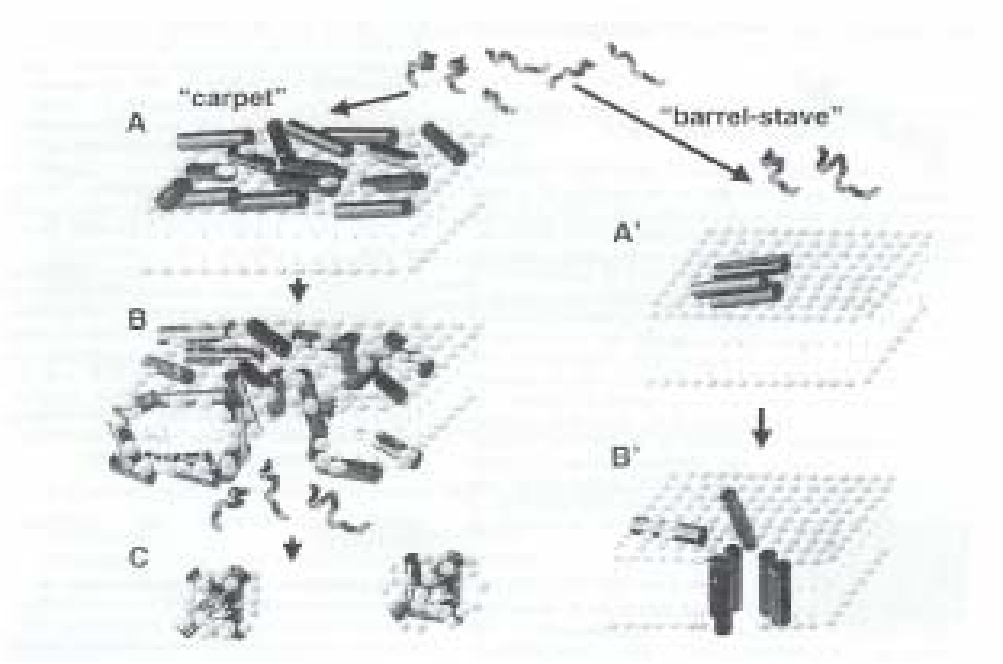

Figure 5: The detergent (carpet) and barrel mechanism

The amphipathic nature and natural activity of LL-37 make this an excellent candidate for drug studies. The positive portion attracts it to bacterial membranes, and the hydrophobic portion can then penetrate the lipid membrane. The preliminary results suggest that its salt-resistant antimicrobial activity, significant resistance to proteolytic degradation, aggregation state, structural stability, and predicted N-terminal structure differ from the well-studied antimicrobial peptides of this class, such as *Leptospira interrogans*, *Borrelia*, and *Treponema pallidum* (7). These differences affect features critical to the proposed pore model shown in figure 5, and suggest a unique mechanism for LL37. (2)

The sequence of this synthetically prepared fragment of the human antimicrobial peptide LL37 is RKSKEKIGKEFKRIVQRIKDF (Figure 6). The LL-21 sequence was chosen by cutting each amino acid from the N and C terminus and checking its activity. This then allowed our collaborators to discover the most important sequence which was the amino acids 1-21 on the N-terminus (8). LL37 is a member of the cathelicidin family and has a potently antimicrobial C-terminal domain. It has a distinct α-helical conformation, especially if near negatively charged lipids. It also has been shown to help in recruiting cellular immune response as a chemoattractant (9). These characteristics indicate that the LL21 fragment is capable of antimicrobial activity. Developing a shorter sequence than parent is economically and synthetically advantageous as discussed in the first project.

Previously to obtain information on lipid specificity our collaborators at U of M measured the attraction to different types of cell membrane model liposomes using fluorimetry experiments. This suggested that the peptide was more attracted to the negatively charged model over the neutral or positively charged forms.

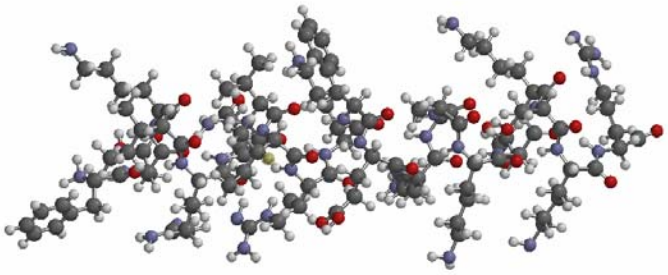

RKSKEKIGKEFKRIVQRIKDF

Figure 6: The LL-21 structure shown as a ball and stick model. The positively charged Arg (R) and Lys (K) residues confer specificity for bacterial membranes.

This study might give way to other drugs based on amphipathic peptides and help people who are immune deficient. Also, antimicrobial peptides may be of special interest in the dental fields, as they are found in mucosal epithelial cells; their activity can help against oral disease, such as *P. gingivalus*.(11) Furthermore, if used in combination with other antibiotics, they may have a synergistic effect on the body. There is also a demand for new antibiotic drugs that cannot progress to become resistant to infectious organisms. These peptides inhibit the growth of both Gram-positive and Gram-negative bacteria (12)

Materials and Methods

Each amino acid in the sequence was weighed out at 0.4 mmoles along with 0.152 g (0.4 mmoles) of O-Benzotriazole-N,N,N',N'-tetramethyl-uronium-hexafluoro-phosphate (HBTU, a peptide coupling agent) in separate vials. These were then put into the PS3 protein synthesizer in the sequence of the peptide from the C-terminal to N-terminal residue corresponding to the specified analog of Tendamistat or LL21 peptide.(Figure 7). A vial of acetic anhydride was placed two positions away from the N-terminus to acetylate the Tendamistat peptide for the purpose of keeping the N-terminus from becoming charged. The reaction vessel contained 0.1648 g of Fmoc-Rink Amide MBHA resin (9-fluoronylmethyloxycarbonyl Rink amide methylbenzyhydylamine resin) and a small amount of DMF (N,N-dimethylformamide). This resin results in a carboxamide at the C-terminus after cleavage. The solutions required for synthesizing were 0.4 M DIEA (N,N-diisopropylethylamine/DMF (activator)), and 20% piperidine

(deprotectant) in DMF. The synthesizer was used to attach the terminal amino acid to the solid resin support, and, then it coupled each amino acid by forming amide bonds with the aid of coupling agents, selective deprotectents, and solvent washes. The Tendamistat peptide was programmed for single coupling, while the LL21 analog was double coupled (2 vials of each amino acid at each position). This is because LL21 is a much longer and more difficult sequence than the Tendamistat octapeptide. Also, couplings 5-15 in a sequence tend to be difficult as the longer chain starts to form secondary structures during the synthesis. So double coupling assures completion of each step, resulting in fewer impurities and higher yield.

Figure 7: The PS3 synthesizer.

After the synthesis was completed we performed cleavage and work up of the newly formed peptide. The reaction vessel from the synthesizer was rinsed with methanol, ethanol, and methylene chloride, respectively and then the peptide resin was dried for half an hour under vacuum. Next, we prepared the cleavage cocktail, which had

0.5 ml anisole and 0.5 ml of water in a separate beaker. Since the sequence contained a Trp residue we added 0.5 ml thioanisole. Thioanisole is just another scavenger (phenyl-SCH3) that traps carbocations generated in the cleavage process (since it's an electrophilic aromatic substitution substrate). The Trp side chain indole ring is notorious for having things add back, giving unwanted adducts, so the extra scavenger helps alleviate this. Then we added one crystal of phenol and 10 ml of trifluoroacetic acid to the cocktail. The anisole, thioanisole, and phenol were added because they act as scavengers for any reactive species generated during the cleavage. The cocktail was stirred for about 5-10 minutes on ice before adding this to the resin. The cocktail and resin was covered with parafilm and removed from the ice bath next, this was stirred at room temperature for 1-2 hours and the solution turned yellow.

A side arm flask and filter funnel was set up for pouring, and the cleavage mixture was poured through a filter funnel and collected in a side arm flask. The beaker from which the mixture was poured was washed 2-3 times with miniscule amounts of TFA to ensure quantitative transfer Then 50 mL of cold diethyl ether was added to the TFA solution, slowly while stirring, which caused the peptide to precipitate. Since this is an exothermic reaction it was carried out in an ice bath to maintain temperature and prevent side reactions. Another side arm flask was set up with a fine disc Buchner funnel, and the precipitate in ether was poured in. Then 10 mL of ether was added to the funnel and the precipitate was stirred with a stainless steel spatula. This was done a couple of times to make sure all the thioanisole was removed. The flask was changed and the peptide was dried under water aspirator. Once this was completed, it was transferred to a small lyophilization flask and 70% acetonitrile/H_2O was added. An equal amount of distilled

water was added to the mixture and then it was placed in a dry ice/acetone bath to freeze while rotating. This increased the surface area for lyophilization which took place overnight.

The next step was to perform High Performance Liquid Chromatography (HPLC), which purifies the peptide by removing any leftover scavengers or other impurities that may be present. The peptide was first completely dissolved in a small amount of DMF and loaded into the HPLC machine with a syringe. Gradient program two was run, which is a linear gradient of 10% to 50% acetonitrile (solvent B)/water (solvent A) over two hours. The best peaks were observed and were collected in tubes. These were then lyophilized and an analytical HPLC was used to determine the purity of the peptide. This was the point at which our contribution to the LL-21 peptide research was complete. Collaborators at the University of Michigan continued the project through extensive studies of the LL-21 peptide active. The LL-21 was tested against a variety of gram positive and gram negative bacteria. Some analogs will later be isotopically labeled peptides for solid state NMR studies, providing information on the membrane orientation and mechanism of action.

The last step for the Tendamistat analog was to perform three enzyme assays to determine the activity of α-amylase in the absence and presence of our synthesized inhibitor. Each assay was done in the same way but with varying concentrations of inhibitor (0.1, 0.2, and 0.3 mM) for each trial. The total volume in each tube was 1000 μL, with different volumes of buffer and substrate. The volumes/concentrations of the enzyme and inhibitor/DMSO (DMSO only for the control or the uninhibited tubes) were constant. The substrate (p-nitropenyl- α-D-maltoside) was bought already packaged in a

50 mg vial (bought from Calbiochem, Inc). It was prepared by dissolving it in 2300 μL of Hepes buffer at pH 7. The enzyme preparation of α-amylase (isozyme I, bought from Sigma Corp.) was done by dissolving 46 μL of porcine pancreatic α-amylase in 454 μL of Hepes buffer. The inhibitor concentrations of 0.1, 0.2, and 0.3 mM were prepared by adding 1400 μL of DMSO to 1.01, 2.09, and 3.01 mg of synthesized peptide respectively. There were 7 tubes prepared for the inhibitor and 7 tubes for the uninhibited run (each with a varying amount of substrate) giving a total of 14 tubes. Table one shows the volumes and preparation of each tube.

Table 1: The preparation of each set of tubes for the inhibited and uninhibited runs. The DMSO volume for one set of tubes contains the inhibitor and the other set does not.

Tube	[S] (mM)	Substrate Volume (μL)	Buffer Volume (μL)	Enzyme Volume (μL)	DMSO Volume (μL)
#1	1.0	20	783.9	29.4	166.7
#2	3.0	60	743.9	29.4	166.7
#3	5.0	100	703.9	29.4	166.7
#4	8.0	160	643.9	29.4	166.7
#5	10.0	200	603.9	29.4	166.7
#6	13.0	260	543.9	29.4	166.7
#7	16.0	320	483.9	29.4	166.7

By varying the volume of the substrate and buffer, the concentration of the substrate added each time was different even though the total volume remained the same. The order of adding the substrate, enzyme, buffer and DMSO was crucial for reading absorbance's during the spectroscopy study because if not put in order the enzyme might denature. The enzyme was added first, followed by the buffer and then the DMSO. The tubes were incubated for 30 minutes without the substrate, at 30˚C After incubation, the tube was taken out to be analyzed by UV/Vis spectroscopy. The substrate was added to a tube, which was then vortexed to ensure complete mixture before placing it in the cuvet

for reading. The UV/VIS spectrophotometer was set at 405 nm, because this is the wavelength at which the product (p-nitrophenolate) has maximum absorbance. The instrument was set to record the change in absorption/concentration of the product of the reaction between the enzyme and substrate for 2 minutes with 10 second intervals between readings. The rates of the increasing absorption/concentration for each tube were recorded and then analyzed using Excel. Beer's Law was used to determine the concentration from the absorbance. Michaelis-Menton and Lineweaver-Burk graphs were made. These plots allowed determination of the V_{max}, K_m, and K_i of each of the three assays and the average K_i for all the assays.

Results

Alpha-amylase results

The results for the α-amylase inhibitor runs are shown first, and then the LL-21 results are given. Both Lineweaver-Burk plots and Michaelis Menten plots are provided for each run in Figure 8 through Figure 13. This illustrates the activity of the enzyme as the concentration of the inhibitor increases by 0.1mM in each reaction. Figure 8 shows the Lineweaver Burk plot of 0.1 mM of the inhibitor, where the inhibited best fit line is steeper as expected. In Figure 9 there is a Michaelis Menton Plot of the inhibitor at 0.1 mM it shows the inhibited run is slightly lower in activity than the uninhibited run and only the fifth point could cause concern (but is probably due to experimental error).

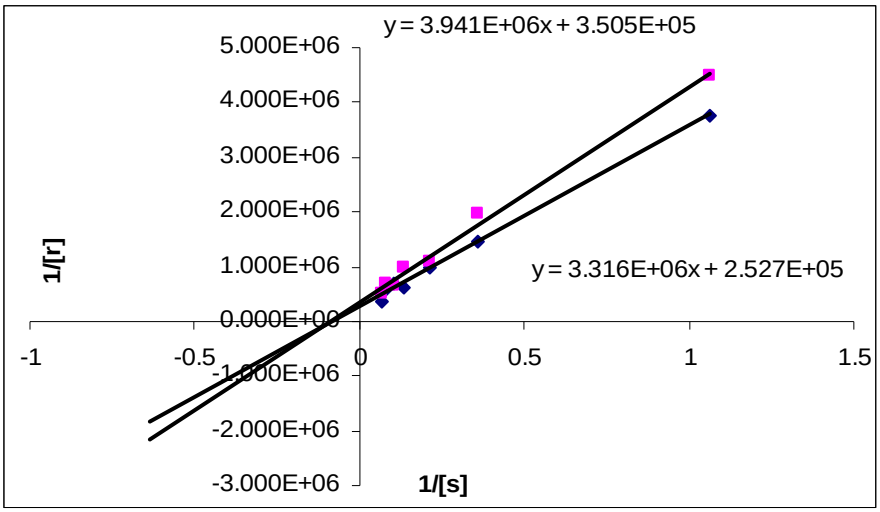

Figure 8: Lineweaver-Burk plot of 0.1 mM of the inhibitor.

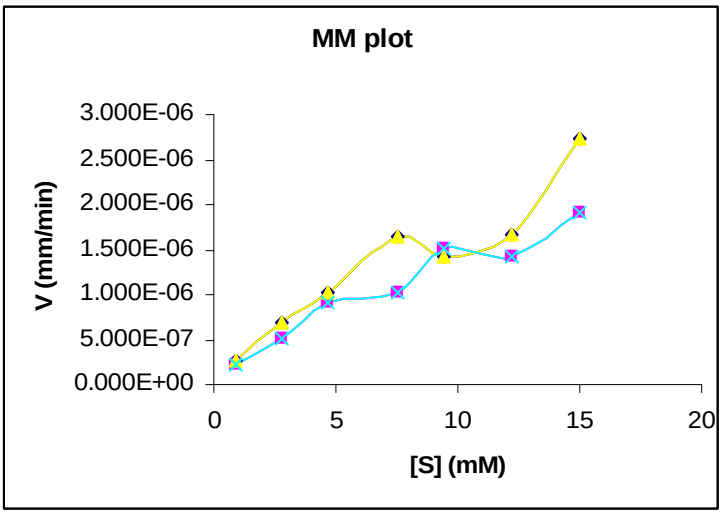

Figure 9: Michaelis Menton plot of the inhibitor at 0.1 mM

Figure 10 and 11 show the Lineweaver-Burk plot and the Michaelis Menton plot respectively for the 0.2 mM run. Some of the points for inhibited run show better activity than uninhibited, but overall, the data show inhibition by the peptide.

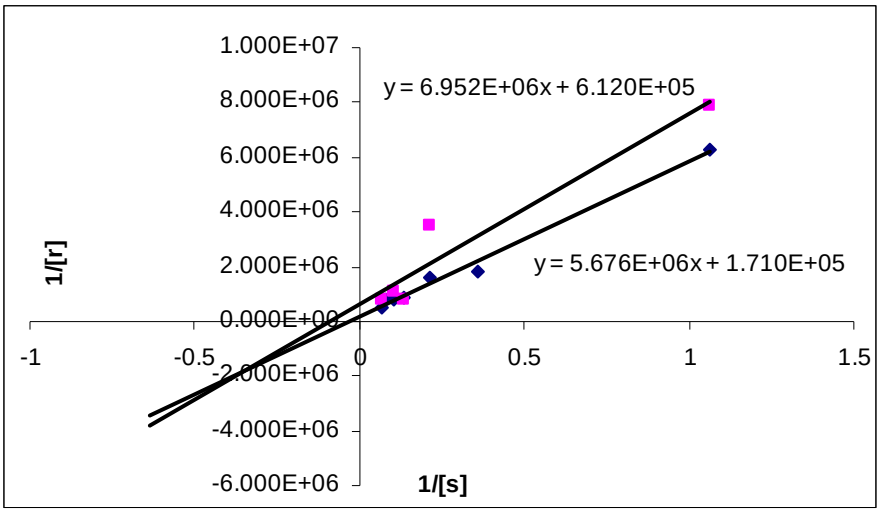

Figure 10: Lineweaver-Burk plot of the inhibitor at 0.2 mM.

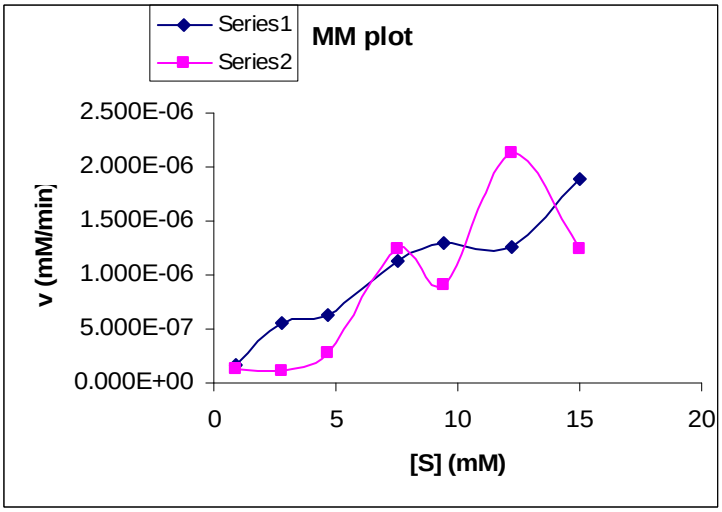

Figure 11: Michaelis Menton plot of the inhibitor at 0.2 m

Figure 12 and 13 are similar to 8 and 9, since the data is consistent with the uninhibited enzyme being of lower activity than the inhibited. Points 4 and 7 are questionable but on the whole, the plots show inhibition.

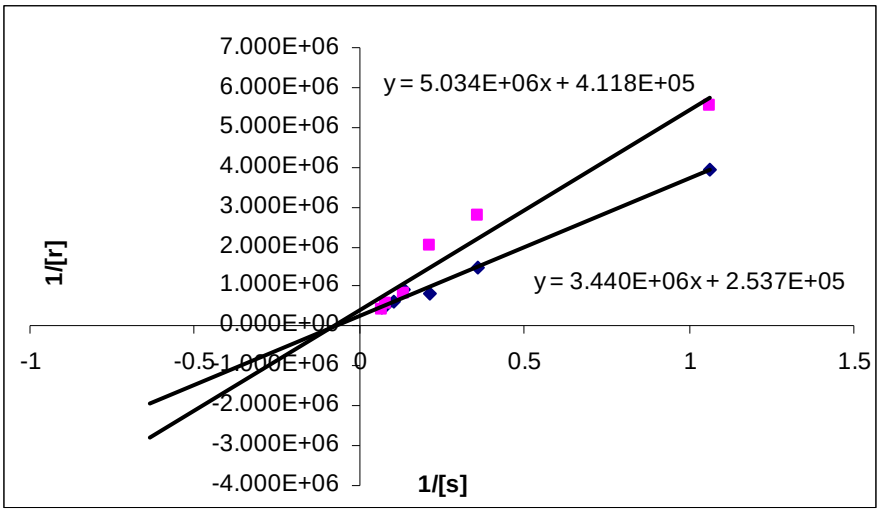

Figure 12: Lineweaver-Burk plot of the inhibitor at 0.3 mM.

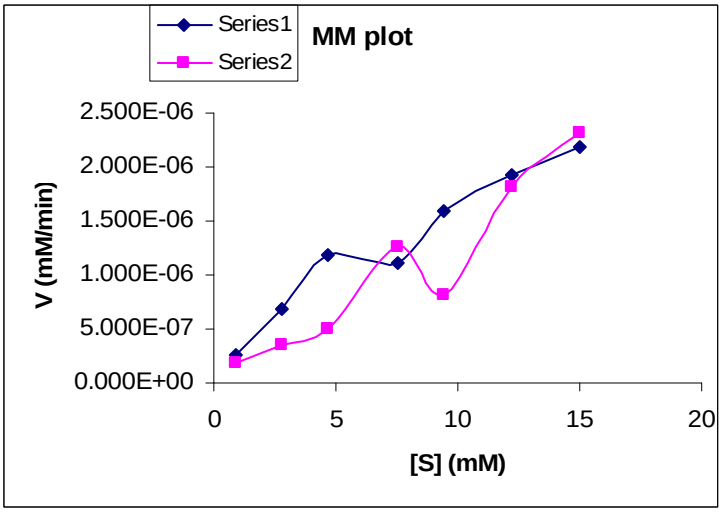

Figure 13: Michaelis Menton plot of the inhibitor at 0.3 mM

Tables 2-4 give the results of the three assays run. The data given is the rate of control runs and the rate of inhibited runs (as measured by an increase in absorbance, indicating increased formation of product) for the amount of substrate added to each vial. Table 2 provides the results for the enzyme with 1 mg of inhibitor and most of the data shows that the control rates are greater than the inhibited ones. Table 3 has the rates of the enzyme at 2 mg of inhibitor and this assay has contradicting data since it shows both

increase and decrease of inhibited in comparison to control. Table 4 is similar to Table 2 with most of its data being consistent with what we would expect.

Table 2: The rates of the enzyme at 1 mg (0.1 mM) of inhibitor

Tube	[S] (mM)	Rate of control (dA/min)	Rate of inhibited (dA/min)
#1	1.0	0.0025	0.0021
#2	3.0	0.0065	0.0048
#3	5.0	0.0096	0.0086
#4	8.0	0.0156	0.0096
#5	10.0	0.0135	0.0142
#6	13.0	0.0158	0.0135
#7	16.0	0.0258	0.0181

Table 3: The rates of the enzyme at 2 mg (0.2mM) of inhibitor

Tube	[S] (mM)	Rate of control (dA/min)	Rate of inhibited (dA/min)
#1	1.0	0.0015	0.0012
#2	3.0	0.0052	0.0011
#3	5.0	0.0059	0.0027
#4	8.0	0.0107	0.0117
#5	10.0	0.0123	0.0086
#6	13.0	0.0091	0.0201
#7	16.0	0.0178	0.0117

Table 4: The rates of the enzyme at 3 mg (0.3 mM) of inhibitor were as follows:

Tube	[S] (mM)	Rate of control (dA/min)	Rate of inhibited (dA/min)
#1	1.0	0.0024	0.0017
#2	3.0	0.0065	0.0034
#3	5.0	0.0112	0.0047
#4	8.0	0.0104	0.0118
#5	10.0	0.0151	0.0077
#6	13.0	0.0182	0.0171
#7	16.0	0.0206	0.0218

Sample Calculations.

V_{max}, K_m, and K_i were determined from the equation of the line given on the Lineweaver-Burk plot. We used V_{max} and K_m for uninhibited/control runs and prime values (V_{max}' and K_m') for inhibited.

0.1mM Inhibitor

Uninhibited

V_{max} = 1/y-int = 1/3.55 X 10^{05} = 2.853 X 10^{-06} M/min

Inhibited

V'_{max} = 1/ 2.527 X 10^{05} = 3.960 X 10^{-06} M/min

Uninhibited

K_m= slope * V_{max} = (3.941 X 10^{-06})(2.853 X 10^{-06}) = 11.24 mM

Inhibited

K'_m = (3.316 X 10^{-06})(3.96 X 10^{-06}) = 13.13 mM

Ki : inhibited m = uninhibited slope (1 + ([I]/Ki)

Ki =0.53 mM = 531 μM

This was then done for the two other assays and the results for those follow.

0.2 mM inhibitor

V_{max} =9.132 X 10^{-06} M/min

V'_{max} = 5.848 X 10^{-06} M/min

K_m = 6.975 mM

K'_m = 32 mM

K_i = 0.579 mM= 579μM

<u>0.3 mM inhibitor</u>

Vmax = 2.120 X 10^{-06} M/min

V'max = 3.941 X 10^{-06} M/min

Km = 10.55 mM

Km' = 13.56 mM

Ki = 0.647 mM= 647μM

Average Ki:= ((K_{i1} +K_{i2} + K_{i3})/3) = 0.595 mM = 595μM

Another way to determine K_i is to plot [I] vs the slope of the Lineweaver-Burk plot (Fig 14). The negative of the x-intercept is the K_i. This method gave a K_i of 758 μM which is very close to the averaging method of each individual run.

The parent peptide NFH 1 (Tendamistat 15-22) gives an average K_i of 375 μM (for Tyrosine[1]).

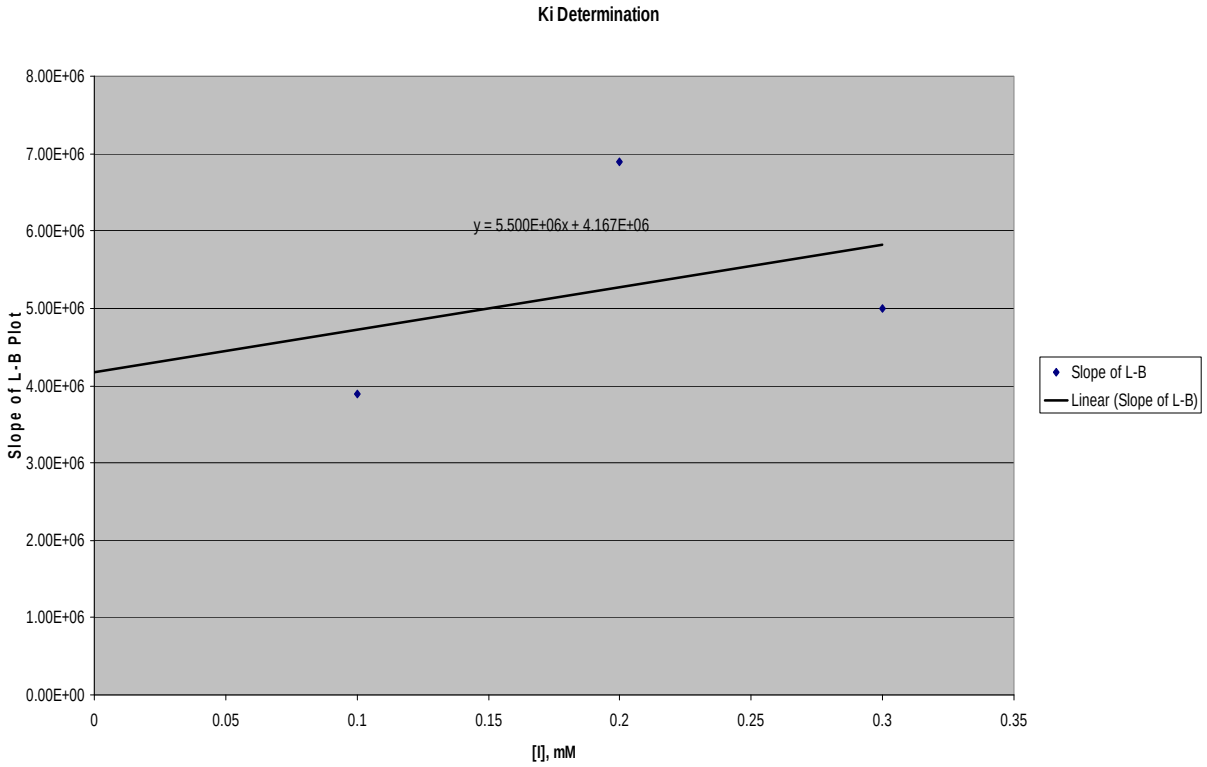

Figure 14: K_I determination plot.

LL-21 Results

In the other experiment (activity determination for LL21) the ability of the peptide to inhibit the bacteria is shown in Table 5, where it gives the minimum inhibition concentration (MIC). Figure 15, the concentration vs. activity plot for S. enterica and S. aureus are a representation of LL-21 activity.

Table 5: Different bactria strains studied to show the minimum inhibitory concentration of LL21. Gram stains (+) or (-) indicated.

Bacterial Strain	**LL21 / MIC (μg/ml)**
Porphyromonas gingivalis W83 (-)	12.5

Staphylococcus aureus (+)	50
Salmonella enterica (-)	50
Pseudomonas aeruginosa (-)	100
S. Gordonia (+)	6.25
Enterococcus feacalis FA2-2 (+)	12.5
Enterococcus feacalis OG1X (+)	50
Escherichia coli (-)	0.4

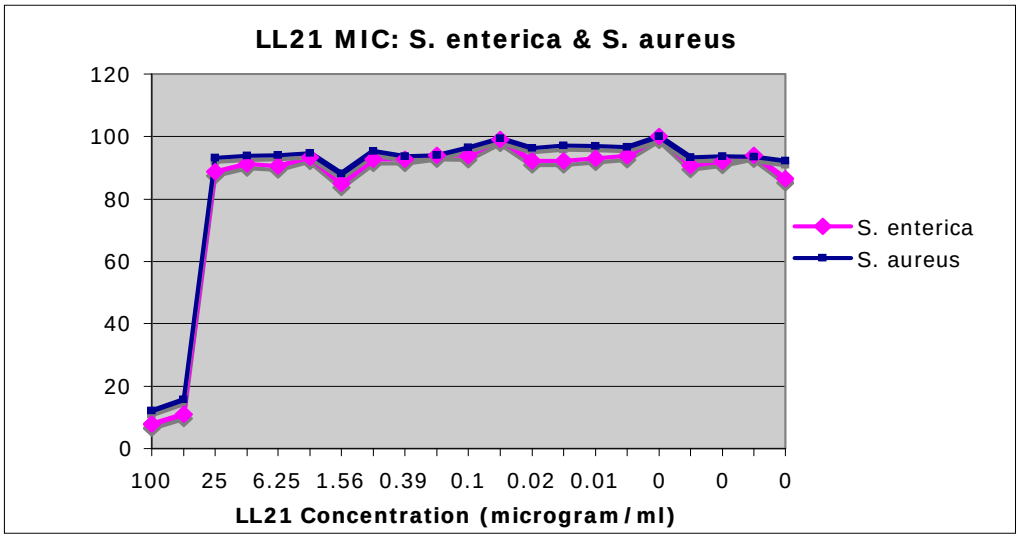

Figure 15: The concentration vs. activity plot for S. enterica and S. aureus as a representation of LL-21 activity.

Discussion

Each assay varied in its results, so the first assay will be discussed first. The Michaelis Menten plot is good for observing the correlation between the inhibited and control curves. This plot allows an estimation of the V_{max} and K_m for each particular assay. Since the parent peptide, Tendamistat, is a competitive inhibitor of α-amylase,

then our peptide should also shows signs of competitive inhibition. The V_{max} and K_m for the uninhibited and inhibited reactions were fairly similar (for 0.1 mM V_{max}=2.85 X 10^{-06} M/min for uninhibited and 3.96 X 10^{-06} M/min for inhibited while K_m for uninhibited is 11.24 mM and 13.13 mM for inhibited.). There was one noted error on the fifth data point by the uninhibited being higher than the inhibited for both runs which could be due to an error in preparation (e.g. substrate or enzyme not mixed well before addition to each tube). This could not be repeated due limited peptide, time to re-synthesize peptide, and expense of substrate. Since there is less than a two fold difference in the parameter values, it is not considered a drastic change (only when the magnitude is 10 to 100 fold different is it considered significant). Since the Lineweaver-Burk plot takes the double reciprocal of the data and a best fit line is drawn, it tends to average the points so that one bad point does not often grossly influence the plot (Figure 8). This linear plot is considered a better representation of the data obtained. The fact that the lines cross near the origin makes it difficult to determine if the inhibition is competitive or noncompetitive, which is likely due to insensitivity in our assay. This run appears to show competitive inhibition because the lines intersect near the y-axis, but not close enough to be certain. The calculations to determine the V_{max}, K_m and K_i were performed using the equation of the line as shown previously. The V_{max} for the uninhibited and inhibited runs were extremely close. The K_m for the two trials was fairly close. The K_m for the inhibited run was slightly lower than that of the uninhibited one, which is not expected for competitive inhibition; however, the values are not significantly different which simply indicates that inhibition is weak. In conclusion the data for this assay did correlate with the hypothesis even though one point was misleading, which could be due

to an error in the experiment. The dA/min is decreasing for each inhibitor tube which shows that there is inhibition taking place in the tubes. This run could be repeated in the future to ensure accurate interpretation of results.

The second assay exhibited about the same V_{max} values even though there were a couple places where the curves crossed each other in the Michaelis-Menten plot (Table 3 and Figure 11). An error could have occurred in not using the Pipetman pipettor accurately. Upon analysis of the Lineweaver-Burk plot, the reaction exhibited inhibition, this time with lines crossing closer to the x-axis, an indication of non-competitive inhibition. The calculated V_{max} values again are very similar values, where there is about a 36% difference. This is only a less than 2- fold difference in magnitude, however, and not considered significant. The K_m did show an increase for the inhibited run (32 mM versus about 7 mM , almost a 5-fold change), another indication of non-competitive inhibition, although weak.

The final assay was similar to the first assay and the Michaelis Menten plots were fairly similar with only two odd points. The values for V_{max} and K_m respectively for the inhibited were 3.94 X 10^{-06} M/min and 13.56 mM while the uninhibited values were 2.12 X 10^{-06} M/min and 10.55 mM. The Lineweaver-Burk plot exhibited the lines intersecting slightly to the left of the y-axis, but above the x-axis (type of inhibition inconclusive). The calculated V_{max} values were fairly close which can indicate competitive inhibition (uninhibited was actually14% lower than inhibited), and the K_m was slightly increased for the inhibited run relative to the uninhibited run. Still, the values were very similar between assays, indicating weak inhibition.

In conclusion, inhibition took place but the data was not conclusive as to which type. Also comparing K_i values for the parent peptide (NFH-1) and our synthesized peptide, the value for our analog is higher (ave. 595 μM versus 375 μM for NFH-1, lower values indicating better inhibition), indicating weaker interaction with the enzyme. This showed that this is not in the desired nanomolar range for drug development and it has poor activity. Since $–NH_2$ and -OH are very similar in size, electronic character, and the ability to act as both H-bond donors and acceptor, differences in activity between the analogs is surprising. Still, the difference is less than 2-fold so not considered significant. This sequence should either be assayed again to confirm the data or it could be modified slightly to give better activity results. These results were somewhat inconsistent and it was hard to determine what was occurring except that inhibition was taking place for the most part. In future trials it might be good to conduct these assays sequentially right after each other to ensure that the conditions are the same for each trial (pressure, temperature, concentrations, etc). An alternate assay may also be developed.

The second experiment that I worked on was with the LL-21 peptide which showed promising activity. The newly synthesized peptide required only slightly higher concentrations compared to the parent LL37 to inhibit bacterial growth. Given its shorter sequence, this is impressive. The best activity shown was against *E. coli* since its MIC was 0.4 μg/mL, and any concentration below 10 μg/mL is useful. In the future we will examine the three-dimensional structure of our analog and orientation with respect to the membrane with NMR (with isotopic labels present for NMR studies) to give more information on the exact mechanism of action. This is a good potential mechanism to

treat infections with excellent societal implications since it may lead to the development of an antibiotic to which the bacteria cannot develop resistance.

References

1) http://72.14.203.104/search?q=cache:4Kvjiz7M5AgJ:www.gsr.emich.edu/_pages_grad/gradstudents/gradstudents_subdir/researchfair/researchfair_subdir/resfair_2003/2003_subdir/g_2003_abstracts.html+alpha+amylase+and+diabetes+streptomyces&hl=en

2) http://www-nmr.cabm.rutgers.edu/photogallery/proteins/htm/page17.htm

3) Pflugrath,J.W., Wiegand,G., Huber, R. and Vertesy, L. (1986) Crystal Sturcure determination, Rifinement and the Molecular Model of the Inhibitor HOE 467A. J. Mol. Biol. **189**, 383-386

4) Kline, A.D., Braun, W. and Wuthrich, K. (1988) Determination of the Complete Three-Dimensional Stucture of the α-amylase Inhibitor Tendamistat in Aqueous Solution By Nuclear Magnetic Resonance and Distance Geometry. J. Mol. Biol**. 204**, 675-724

5) Dr. Heyl-Clegg research plan on α-Amylase , 2004.

6) Wiegand, G., Epp, O. and Huber, R. (1995) The Crystal Structure of Porcine Pancreatic α-amylase in Complex with the Microbial Inhibitor Tendamistat. J. Mol. Biol **247**, 99-110

7) http://jac.oxfordjournals.org/cgi/content/abstract/50/6/895

8) Dr. Heyl-Clegg (2004), Development and Study of Antimicrobial Peptides as Potential Nonresistant Antibiotics, Department of Chemistry at Eastern Michigan University, Research paper, 1-9

9) http://64.233.167.104/search?q=cache:6xWF4i2hZCkJ:www.phoenixpeptide.com/Catalog%2520Files/LL37/LL37.htm+LL-37&hl=en&gl=us&ct=clnk&cd=1

10) http://www.ncbi.nlm.nih.gov/entrez/query.fcgi?cmd=Retrieve&db=PubMed&list_uids=7542349&dopt=Abstract

11) Y. Shai, From Innate Immunity to de-Novo Designed Antimicrobial Peptides, *Curr. Pharm. Design* **8** (2002) 715-725.

12) Nakamura, T., Furunaka, H., Miyata, T., tokunaga, F., Muta, T., Iwanaga, S., Niwa, M., Takao, T., and shimonishi, Y. (1988). *Tachyplesin, a class of antimicrobial peptide from the hemocytes of horshoe crab*. Isolation and Chemical Structure. J. Biol. Chem. **263** 16709-16713